

SELF-CENTERING CONNECTIONS FOR TRAFFIC SIGN SUPPORTING STRUCTURES

ALDOT Project 930-865R

Final Report

By

Dr. Ying-Cheng Lin
Assistant Professor of Structural Engineering
University of Alabama in Huntsville

S. Vahid
Graduation Student
University of Alabama in Huntsville

March 29, 2015

ACKNOWLEDGEMENTS

The research presented in this report is based on work supported by the Alabama Department of Transportation (ALDOT) under the project No. 930-865R. Any opinions, findings, and conclusions or recommendations expressed in this material are those of the author and do not necessarily reflect the views of the ALDOT.

CONTENTS

LIST OF FIGURES	iii
1 INTRODUCTION	1
2 SELF-CENTERING CONNECTION CONCEPT	1
2.1 Targeted Design Features.....	1
2.2 Self-Centering Connection Conceptual Behavior	1
2.3 Self-Centering Connection Moment Development.....	2
2.4 Self-Centering Connection Energy Dissipation Ratio	3
3 SC CONNECTION DESIGN CRITERIA DEVELOPMENT	4
4 PROTOTYPE STRUCTURE	4
5 BEHAVIOR OF SC-BMS	5
5.1 Computational Analysis Model Description	5
5.2 SC Connection Response: Monotonic Pushover Analysis.....	7
5.3 SC Connection Response: Cyclic Push Analysis.....	8
5.3.1 Self-Centering Behavior	9
5.3.2 Energy Dissipation Ratio	9
6 SC-BMS Global Response.....	10
7 SC AND CONVENTIONAL BMS RESPONSE COMPARISON.....	11
7.1 Initial Stiffness	11
7.2 Damage Inhibition.....	11
7.3 Potential Collapse Prevention	11
7.4 Stabilized Ductility.....	11
7.5 Resilience	12
8 SUMMARY AND CONCLUSIONS	12
9 FUTURE WORKS.....	13
REFERENCES	13

LIST OF FIGURES

Fig. 1 Conceptual SC connection details	2
Fig. 2 Conceptual behavior of SC connection	2
Fig. 3 SC connection gap opening	3
Fig. 4 Free body diagram for overturning moment.....	3
Fig. 5 Energy dissipation ratio effects on self-centering connection $M-\theta_r$ response	3
Fig. 6 Typical bridge mounted structure supporting dynamic message sing.....	4
Fig. 7 Bridge mounted structure schematics: (a) plan, (b) front-view elevation, (c) side-view elevation, and (d) footing (<i>courtesy of ALDOT division 1 and Thompson Engineering</i>).....	6
Fig. 8 Schematics of SC-BMS: (a) before and (b) during rocking	7
Fig. 9 Model for SC-BMS: (a) three dimensional and (b) side view.....	7
Fig. 10 Monotonic pushover SC-BMS connection $M-\theta_r$ response	8
Fig. 11 Rocking motion of SC-BMS model during monotonic pushover	9
Fig. 12 Cyclic push SC-BMS connection $M-\theta_r$ response	9
Fig. 13 SC-BMS $V_{\text{base}}-\theta_{\text{drift}}$ response.....	10
Fig. 14 Comparison of $V_{\text{base}}-\theta_{\text{drift}}$ response for SC and conventional BMSs.....	12

1 INTRODUCTION

Steel structures supporting traffic sign panels are designed as intended to dissipate energy by yielding structural members during severe wind loading (ex. strong hurricanes). Yielding results in inelastic deformations, which are permanent damage to structural members. Structures with permanent deformations present the out-of-plumb appearance. Damage might be repairable; however, deconstruction and replacement of an off-centered structure with a new structure is usually more economical. If a new design approach that controls damage and avoids replacement can be developed, the direct and indirect costs of post-extreme-wind repair for traffic sign supporting structures can be saved enormously.

At present, the design approach mitigating damage for traffic sign supporting structures under extreme wind loads are undeveloped. This research conducts an exploratory study on the new design method of “*self-centering connections*,” termed “*SC connections*.” The scopes of this research project are: (1) design equations and criteria development; and (2) validation through numerical analyses.

2 SELF-CENTERING CONNECTION CONCEPT

2.1 Targeted Design Features

The new design approach is expected to upgrade traffic sign supporting steel structures with the following features:

- (a) Energy dissipation is provided by cost-effective devices, not by member permanent deformations;
- (b) Elastic stiffness and strength are similar to conventional structures;
- (c) Connection gap opening enables relative rotations without damage to members;
- (d) Forces in post-tensioned bolts close connection gap opening and bring the structure back to its plumb position (i.e., self-centering behavior).

2.2 Self-Centering Connection Conceptual Behavior

The targeted design features as described previously are expected to be the result of the self-centering behavior of bolted connections. Fig. 1 illustrates a conceptual example of the application of SC connections at the base of a traffic sign supporting structure. The base plate-support connection is pre-compressed by post-tensioned bolts, and energy dissipation devices (EDs) are added to the connection. The SC connection conceptual behavior is presented by the overturning moment-relative rotation ($M-\theta_r$) response as shown in Fig. 2. When the overturning moment reaches the impending gap opening overturning moment (M_{IGO}), the softening behavior at point A occurs. After point A, a gap opening develops at the base plate-support interface as shown in Fig. 3, which initiates the relative rotation (θ_r). Note that this rotation is not a result of permanent

deformations or damage to structural members. At larger θ_r (point B in Fig. 2), yielding of the post-tensioned bolts might occur, and the secondary softening occurs. Upon unloading at point C in Fig. 2, the overturning moment reduces by twice of the moment contributed by the EDs (denoted M_{FED}), which is due to the reversal of the force in the EDs. During continuous unloading, energy is dissipated by the EDs shown in Fig. 1. When the moment is completely unloaded (i.e., $M=0$), the force in the post-tensioned bolts closes the gap shown in Fig. 3, resulting in zero residual θ_r (i.e., $\theta_r=0$) response in Fig. 2 and bringing the structure back to plumb position (i.e., *self-centering* behavior).

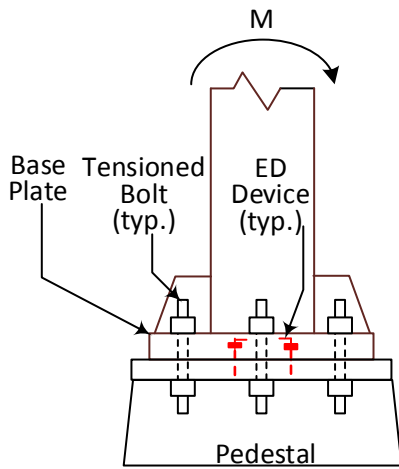


Fig. 1 Conceptual SC connection details

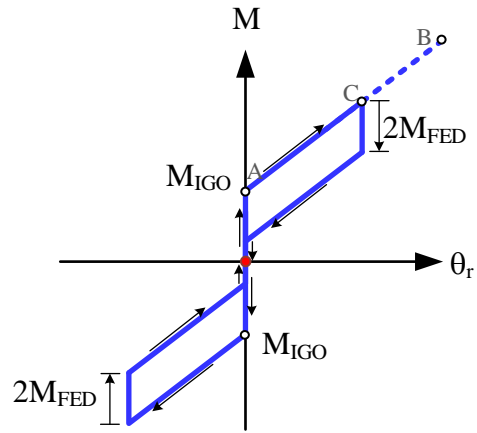


Fig. 2 Conceptual behavior of SC connection

2.3 Self-Centering Connection Moment Development

Using the free body diagram shown in Fig. 4, when summing the moment at the pivot point O, the moment equilibrium equation gives the overturning moment M equation as follows:

$$M = P d_1 + F_{ED} d_1 \quad (1)$$

where P is the axial force in the member; d_1 is the distance between the force P and the point O; F_{ED} is the force resultant in the ED. It should be noted that P includes the post-tensioned bolt force resultant (T_b), the total self-weight of the structure and the attached components (P_{sw}); and P can be expressed as follows:

$$P = T_b + P_{sw} \quad (2)$$

From Eq. (1) and (2), M_{IGO} can be derived as follows:

$$M_{IGO} = (T_{bo} + P_{sw}) d_1 + F_{ED} d_1 \quad (3)$$

where T_{bo} is the total initial force in the post-tensioned bolts. The last term in Eq. (3) is the moment contributed by the EDs, which is denoted M_{FED} in Fig. 2 and can be expressed as follows:

$$M_{FED} = F_{ED} d_1 \quad (4)$$

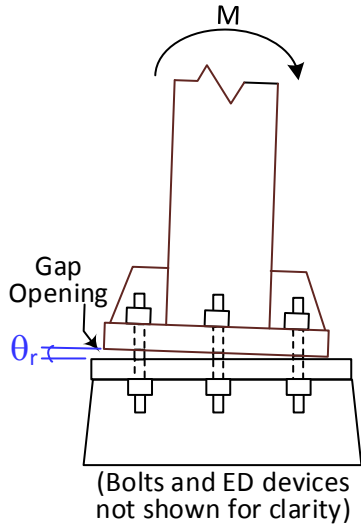


Fig. 3 SC connection gap opening

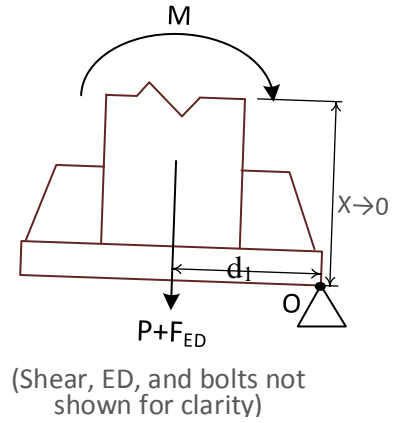


Fig. 4 Free body diagram for overturning moment

2.4 Self-Centering Connection Energy Dissipation Ratio

The energy dissipation ratio (β_E) of the self-centering connections is defined by the follows:

$$\beta_E = M_{FED} / M_{IGO} \quad (5)$$

As illustrated in Fig. 5, β_E effects self-centering behavior. The larger the β_E value, the greater the energy is dissipated by the EDs. However, when the β_E ratio is greater than 0.5 (Fig. 5 (d) and (e)), a connection will not return to zero relative rotation when completely unloaded, and self-centering behavior can not be achieved. Thus, the β_E ratio should be greater than zero for effective energy dissipation, but must be less than 0.5 to enable self-centering behavior as shown by Fig. 5 (b) and (c).

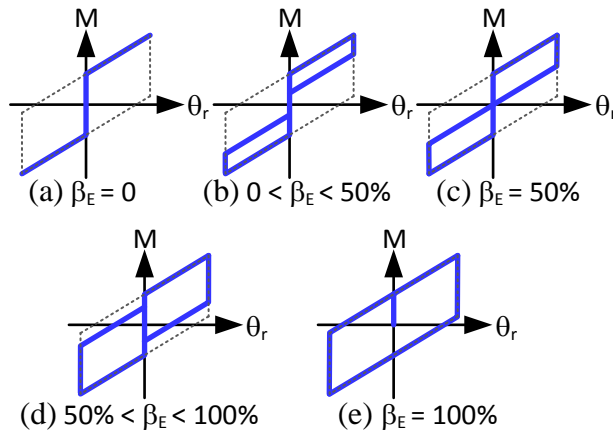


Fig. 5 Energy dissipation ratio effects on self-centering connection M - θ_r response

3 SC CONNECTION DESIGN CRITERIA DEVELOPMENT

A traffic sign supporting structure with SC connections at the base is designed to act like a conventional structure under the design wind load. The major softening behavior at M_{IGO} is expected to occur under the design wind load. Thus, the following design criterion for the SC connection should be satisfied:

$$M_{IGO} = M_{des} \quad (6)$$

where M_{des} is the design overturning moment, which can be determined from a conventional structure (i.e., with fixed connections at the base) subjected to the design wind load per AASHTO (2013).

Based on the previous discussion on the β_E ratio effecting self-centering behavior, the following criterion can be arrived:

$$0 < \beta_E < 0.5 \quad (7)$$

Once a β_E ratio that satisfies Eq. (7) is selected and the M_{IGO} value is determined from Eq. (6), M_{FED} can be calculated from Eq. (5). From Eq. (4), F_{ED} can thus be determined if d_1 is known. By substituting Eq. (6) into Eq. (3), T_{bo} can be determined with known values for d_1 , F_{ED} , and P_{sw} .

4 PROTOTYPE STRUCTURE

For verification of the design concept and criteria described previously, an existing conventional structure was adopted as the prototype structure. This structure is a bridge mounted structure (BMS) that locates in Montgomery, Alabama and supports dynamic message signs, a typical structure of which is shown in Fig. 6.



Fig. 6 Typical bridge mounted structure supporting dynamic message sing

Details of the conventional BMS are schematically presented in Fig. 7. The key dimensions include: the total span (Fig. 7 (a) and (b)) of 137.5 ft; the total height from the base to the center of the horizontal core truss subassembly (Fig. 7(b)) is 22.8 ft; the centerline-to-centerline width of the upright tower truss subassemblies (Fig. 7(c)) is 5.5 ft. The upright tower truss subassemblies are anchored on the pedestals as shown in Fig. 7(d). Steel tubes made of ASTM A500 consist the

horizontal core and the upright tower truss subassemblies; the nominal yield stress is 52 ksi, and the nominal ultimate stress is 60 ksi. The steel tube cross-sectional areas of the horizontal core truss subassembly include 1.3 in² (for the chords in Fig. 7 (a)), 0.21 in² (for the diagonals in Fig. 7 (a) and (c)), and 0.17 in² (for the verticals in Fig. 7 (a) and (c)). The steel tube cross-sectional areas of the upright tower truss subassemblies are 2.49 in² (for the verticals in Fig. 7 (c)) and 0.45 in² (for the diagonals and the horizontals in Fig. 7 (c)).

Using the previously described design criteria and equations, SC connections were designed. $\beta_E=0.4$ is selected for this BMS, which satisfies the β_E criterion presented by Eq. (7). M_{des} of this conventional BMS is determined from an accurate elastic analysis using SAP2000 with a model for the conventional BMS (i.e., the MBS with fixed supports at the bases) subjected to the member self-weight and the design wind pressure per AASHTO (2013). M_{des} is found equal to 2183 kip-in. From Eq. (6), M_{IGO} is set equal to M_{des} . From Eq. (5), M_{FED} is then determined equal to 837 kip-in. At the base of the BMS, SC connections are added as illustrated in Fig. 8 (a), where post-tensioned threaded rods are added to the BMS by extending the anchor bolts from the pedestals, and EDs connect the pedestals to the vertical members of the upright tower truss subassembly. The anchor bolts-to-post-tensioned rods interface are assumed using couplers that are commonly used in practice for threaded rod splicing. The EDs for this prototype are assumed to be friction devices. When M_{des} is reached, the BMS with SC connections at the base (denoted SC-BMS) will open a gap at the base of one pole, pivot on the base of the other pole, and create a controlled “rocking motion” as shown in Fig. 8 (b). From Fig. 8 (b), d_1 can be determined. Using Eq. (4), the magnitude of F_{ED} is calculated equal to 13 kips. Lastly, from Eq. (3), T_{bo} equal to 20 kips can be determined using the known values of all other variables.

5 BEHAVIOR OF SC-BMS

5.1 Computational Analysis Model Description

A nonlinear analysis model for the SC-BMS was built using the structural analysis software SAP2000. This SC-BMS model is a three dimensional model as shown in Fig. 9(a). As shown in Fig. 9(b), post-tensioned rods connect the supports and the vertical members of the upright tower truss subassembly. Friction EDs were included in the model and placed between the supports and the bottom of the vertical members of the upright tower truss subassembly. Member and sign self-weights are included in the model. Wind pressure per AASHTO (2013) exerts on all truss members of the SC-BMS and the dynamic message signs, with the wind pressure magnitude varying in heights.

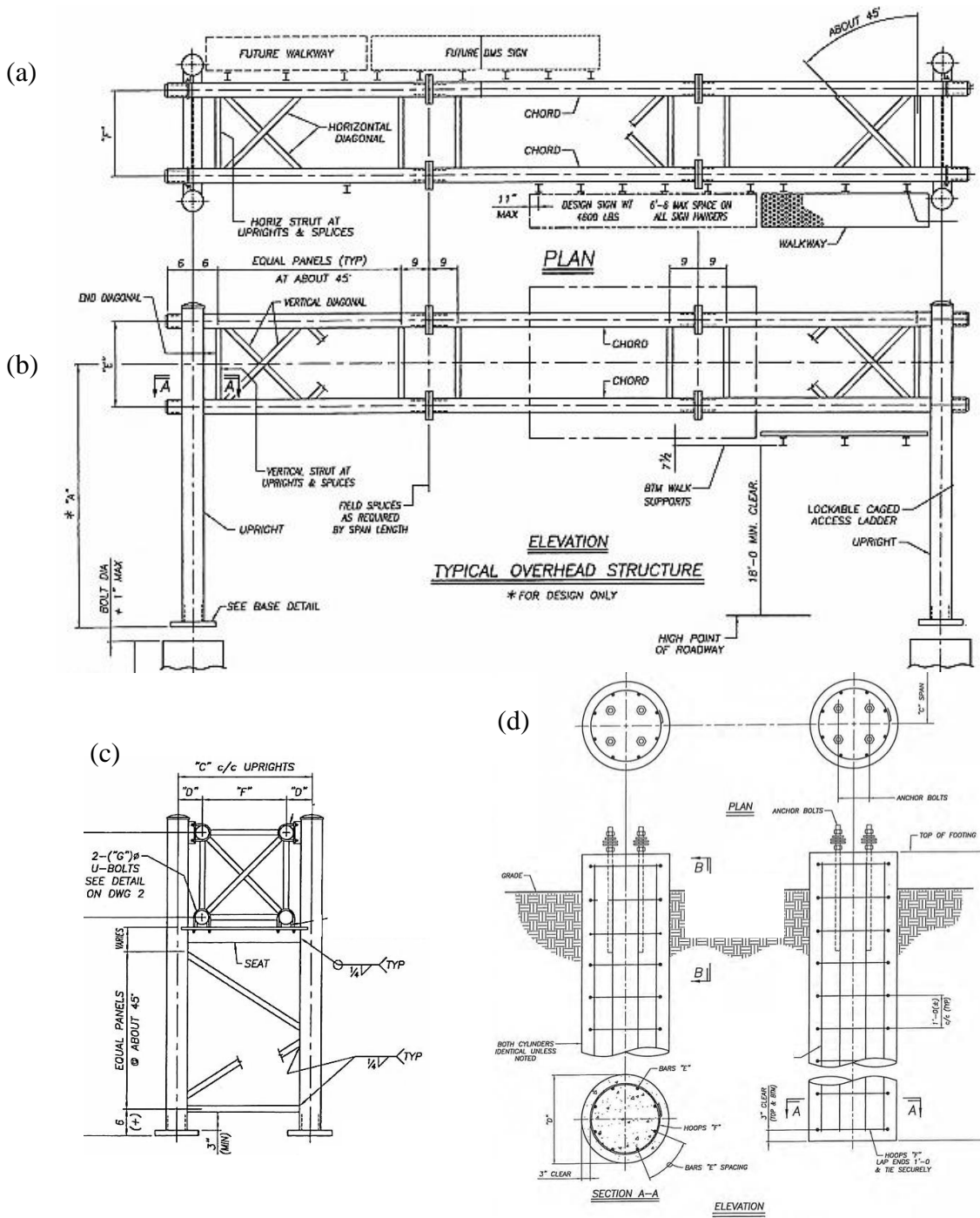


Fig. 7 Bridge mounted structure schematics: (a) plan, (b) front-view elevation, (c) side-view elevation, and (d) footing (courtesy of ALDOT division 1 and Thompson Engineering)

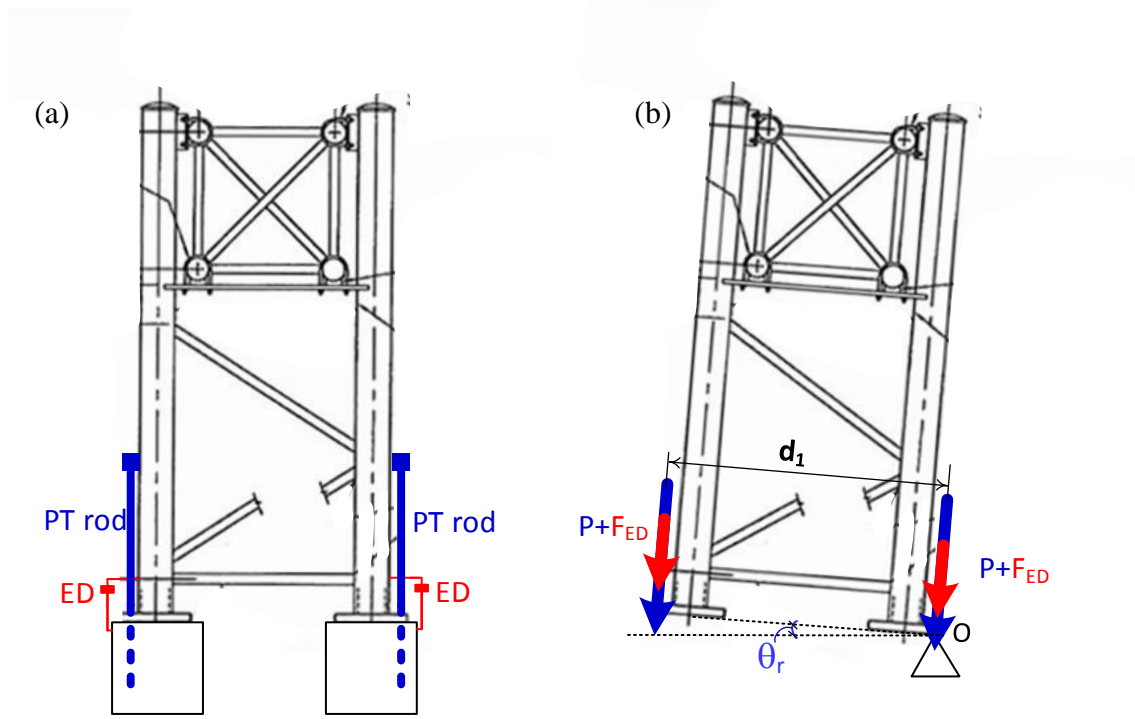


Fig. 8 Schematics of SC-BMS: (a) before and (b) during rocking

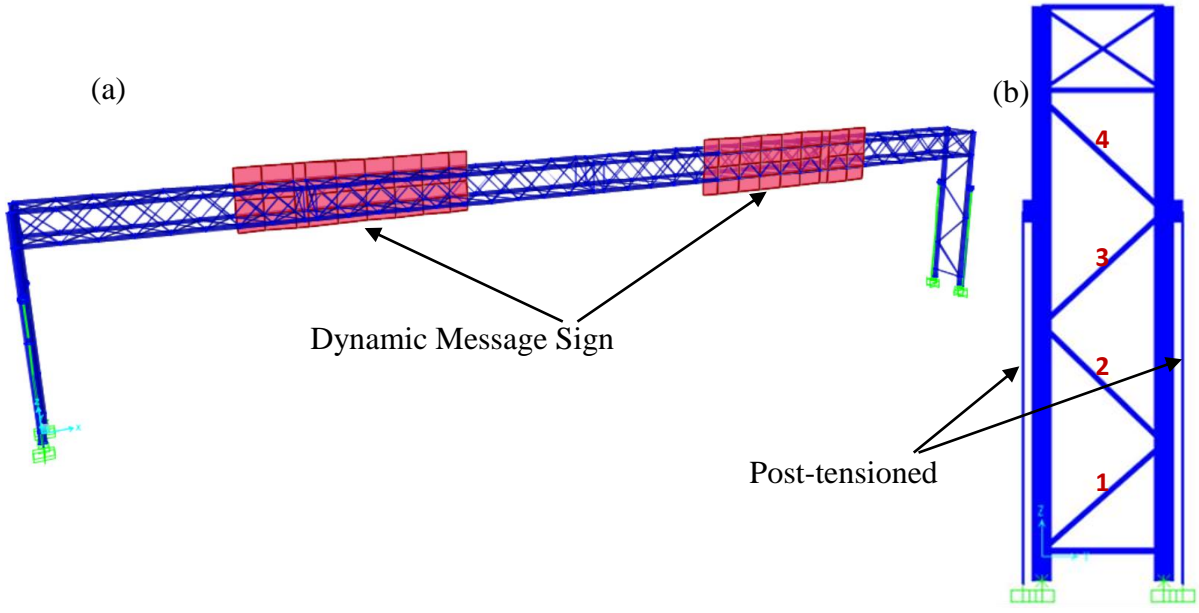


Fig. 9 Model for SC-BMS: (a) three dimensional and (b) side view

5.2 SC Connection Response: Monotonic Pushover Analysis

To study the behavior of the SC-BMS, monotonic pushover analysis was conducted. Fig. 10 presents a typical SC connection M- θ_r response of the SC-BMS from the nonlinear analysis

(denoted NL in Fig. 10). In Fig. 10, M is normalized by M_{des} . At point A, the softening behavior is due to impending gap opening at the tower base which triggers the rocking motion. A typical rocking motion of the SC-BMS during the monotonic pushover analysis is shown in Fig. 11. Note that this softening behavior is not a result of member yielding or damage. At point B, the second softening response occurs, which is due to the modest yielding of only one member of the upright tower truss subassembly (which is the member 3 in Fig. 9(b)). At point C, further softening occurs due to the yielding of the post-tensioned rods.

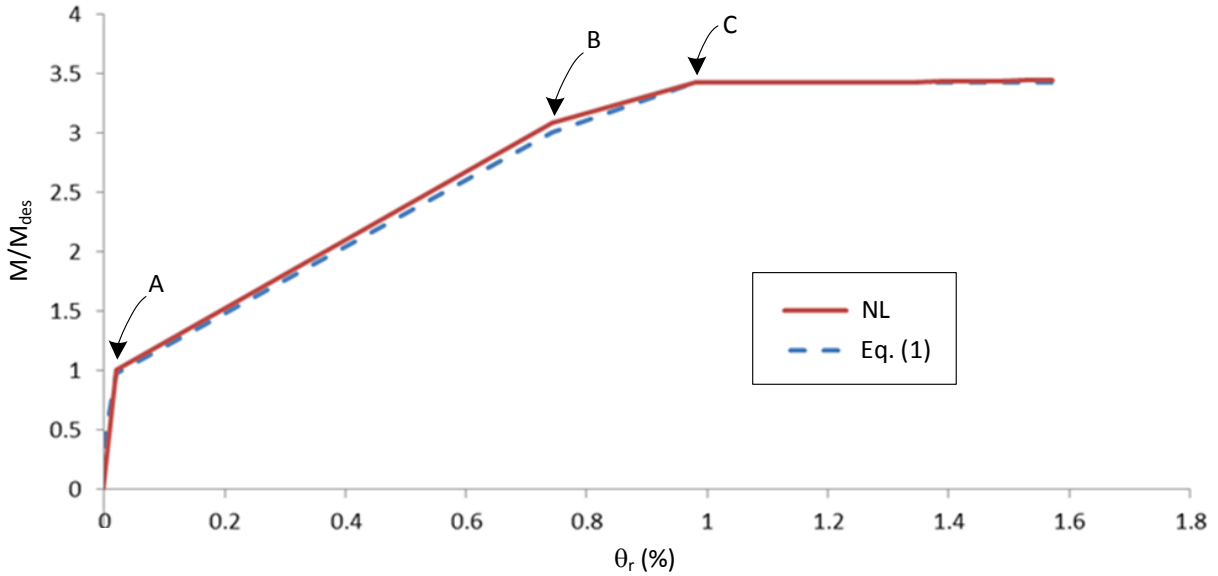


Fig. 10 Monotonic pushover SC-BMS connection $M-\theta_r$ response

For design equation verification, Fig. 10 compares the nonlinear analysis response with the results calculated from Eq. (1). The calculation uses the d_1 value assigned in the model, and the member internal forces from the model for P and F_{ED} as illustrated in Fig. 8 (b). The comparison shows good agreement. Eq. (1) is adequate for overturning moment calculation.

In addition, the first softening point occurs at point A due to impending gap opening at the base when $M/M_{des}=0.98$. This value is very close to 1.0 as targeted by the design criterion of Eq. (6). Thus, this result indicates the adequacy of the design criterion for M_{IGO} of SC-BMSs.

5.3 SC Connection Response: Cyclic Push Analysis

To study the self-centering behavior of the SC connections, cyclic push analyses were conducted on a nonlinear model for the SC-BMS using OpenSees (2013). This software is a nonlinear structural analysis program that has been proved able to provide better accuracy and computational efficiency than SAP2000.

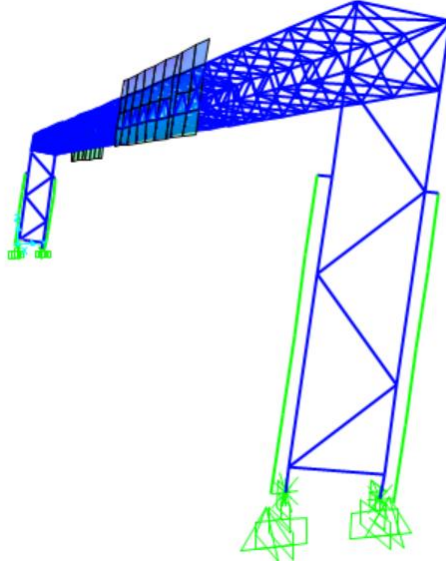


Fig. 11 Rocking motion of SC-BMS model during monotonic pushover

5.3.1 Self-Centering Behavior

Fig. 12 presents the connection $M-\theta_r$ response from the cyclic push analysis. The softening occurs at point A due to impending gap opening at the SC-BMS base without damage to any structural members. After point A, gap opens at the base and the SC-BMS starts to rock on the base. During unloading, hysteretic loops formed, which is due to the non-damage-based energy dissipation from the EDs. The most important observation is at complete unloading (i.e., $M=0$), no residual rotation (i.e., $\theta_r=0$) presents. This indicates the SC-BMS achieved the self-centering behavior as expected by the conceptual behavior shown in Fig. 2.

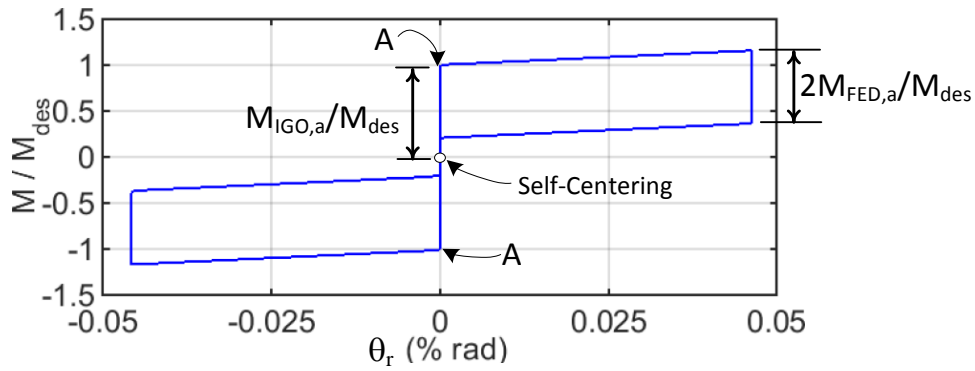


Fig. 12 Cyclic push SC-BMS connection $M-\theta_r$ response

5.3.2 Energy Dissipation Ratio

To study the actual energy dissipation in the SC connection, Fig. 12 and Eq. (5) were utilized for β_E calculation. The analysis result in Fig. 12 that $M_{IGO,a}=0.98M_{des}$ and $2M_{FED,a}=0.79M_{des}$ (or $M_{FED,a}=0.395M_{des}$) were used for M_{IGO} and M_{FED} in Eq. (5) calculating β_E , which led to β_E of the analysis model (denoted $\beta_{E,a}$) equal to 0.403. This $\beta_{E,a}=0.403$ is very close to the design target for

$\beta_E=0.4$ of the prototype structures as previously described on page 5. Thus, the SC connection can be designed to achieve targeted energy dissipation. In addition, the connection with $\beta_{E,a}<0.5$ did self-center after complete unloading, which indicates the design criterion $0 < \beta_E < 0.5$ (i.e., Eq. (7)) is adequate for SC connections to achieve self-centering behavior.

6 SC-BMS Global Response

The global response of the SC-BMS is presented by the result of the normalized SC-MBS lateral drift (θ_{drift}) versus the total base shear (V_{base}) of the SC-BMS shown in Fig. 13. In Fig. 13, V_{base} is normalized by the base shear of the SC-BMS subjected to the design wind pressure per AASHTO (2013) (denoted V_{des}); θ_{drift} is the ratio between the lateral displacement at the mid-height level of the horizontal core truss subassembly and the distance from this mid-height level to the pivot point at the base. At point A, the softening is due to gap opening at the base, and no damage occurs to the SC-BMS. At point B, the softening is due to the yielding in the diagonal members of the upright tower truss subassembly. At point C, the softening is due to yielding in the post-tensioned rods. The occurring sequence of these softening points is similar to what occurred in the base connection response in Fig. 10. Points B and C occurred at larger θ_{drift} in Fig. 13 than θ_r in Fig. 10, which is because θ_{drift} includes the drift contributed by the displacement of members.

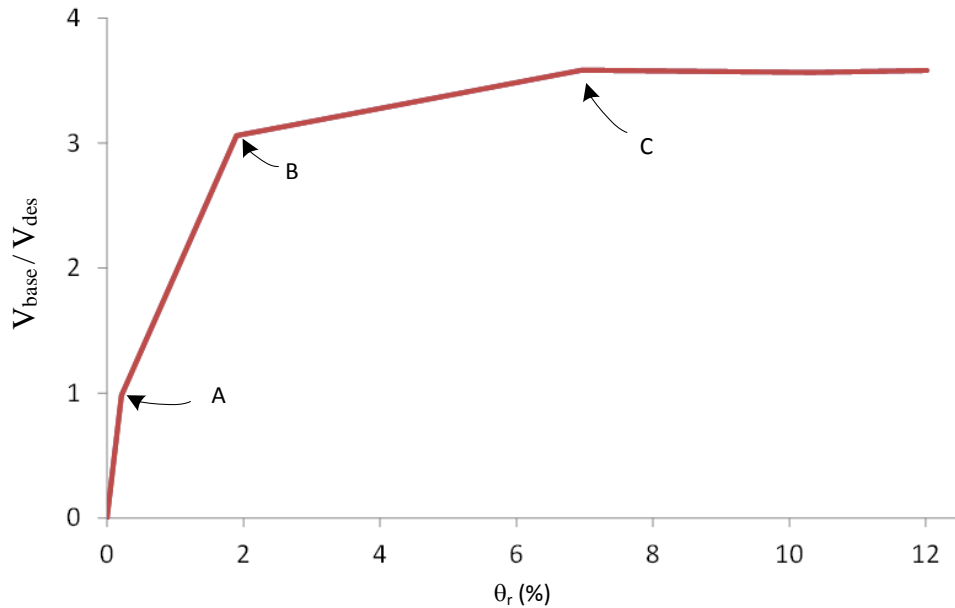


Fig. 13 SC-BMS V_{base} - θ_{drift} response

7 SC-BMS AND CONVENTIONAL BMS COMPARISON

7.1 Initial Stiffness

The advantages of using SC than conventional BMSs can be discovered by the comparison between the two BMS systems. For comparison purpose, a nonlinear analysis model was created using SAP2000 for the conventional BMS shown in Fig. 7. Monotonic pushover analyses were conducted on both models. The normalized $V_{\text{base}}-\theta_{\text{drift}}$ response of the two BMS systems are compared in Fig. 14. The first observation is that the initial stiffness (i.e., the slope prior to point A in Fig. 14) of the two systems is similar, which is as expected by the targeted design features. The point A is the impending gap opening limit state which occurs at the design level wind load. Thus, when subjected to a load smaller than the design wind load, the SC-BMS acts like a conventional BMS, which is the response expected by the previously-described design criteria.

7.2 Damage Inhibition

In Fig. 14, the conventional BMS encounters the first significant softening near the point D, which is due to yielding and deformations in most of the members of the upright tower truss subassemblies. This major softening of the conventional BMS at point D occurs at a very small lateral drift when $\theta_{\text{drift}} = 0.5\%$. In comparison, the yielding of the SC-BMS occurs at point B at larger $\theta_{\text{drift}} = 2\%$. This indicates the SC-BMS system can successfully *inhibit member damage*.

7.3 Potential Collapse Prevention

The second softening of the conventional BMS occurs at point E in Fig. 14, which is due to yielding and deformations of “*all members*” of the BMS (including members of the horizontal core truss subassembly). After point E, the conventional BMS presents a negative stiffness (or slope), which is due to the gravity load effects (or the P-delta effects). This negative stiffness indicates the resistance of the conventional BMS after point E decays and will no longer resist lateral and gravity loads; any further loading would likely collapses the conventional BMS. In comparison, the SC-BMS reaches its maximum strength at point C, but the post-point-C resistance remains constant. Thus, the SC-BMS system provides much better potential of “*collapse prevention performance*” than conventional BMS systems under extreme lateral loads.

7.4 Stabilized Ductility

As shown in Fig. 14, the conventional BMS reaches its ultimate resistance at point E ($\theta_{\text{drift}} = 2\%$) with decaying resistance afterward; while the SC-BMS attains the maximum resistance at point C ($\theta_{\text{drift}} = 7\%$) and remains constant resistance afterward. This comparison indicates the SC-BMS system possesses *higher and more-stabilized ductility* than conventional BMSs.

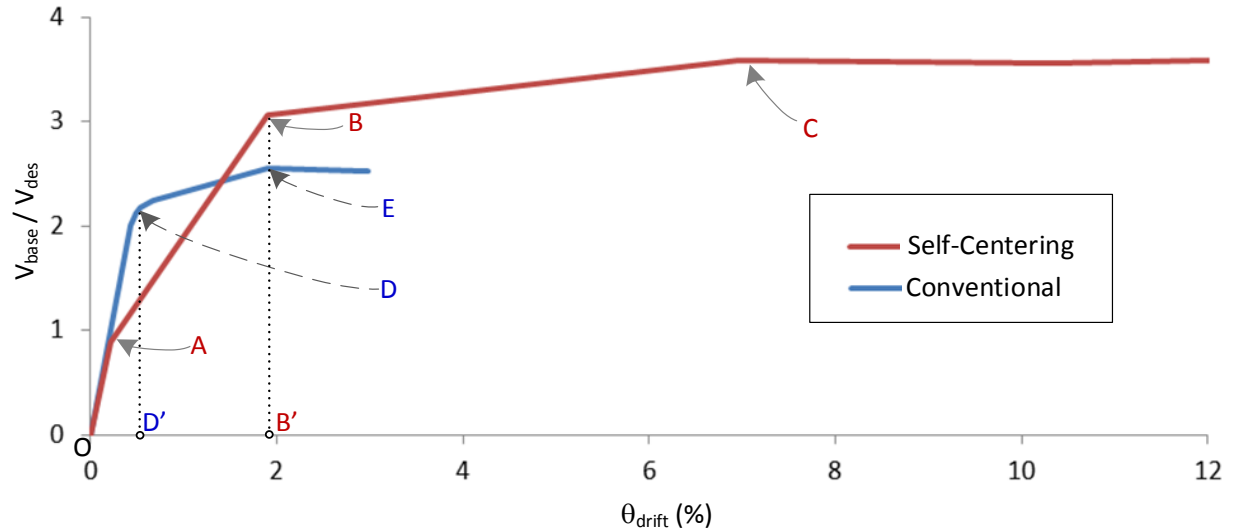


Fig. 14 Comparison of V_{base} - θ_{drift} response for SC and conventional BMSs

7.5 Resilience

The resilience of structural systems in this study is measured by the resilience modulus, which definition can be adapted from the Wikipedia and can be quantified by the normalized maximum energy that can be absorbed by the system without creating permanent deformations. In Fig. 14, the resilience modulus of the conventional BMS can be represented by the enclosed area ODD', which is equal to 0.43. The resilience modulus of the SC-BMS can be represented by the enclosed area OABB', which is equal to 3.4. The resilience of the SC-BMS is about 8 times of the conventional BMS, indicating the SC connections can *significantly improve resilience* of BMS traffic sign supporting structures.

8 SUMMARY AND CONCLUSIONS

This research develops an innovative “self-centering (SC) connection” for traffic sign supporting steel structures to sustain extreme wind loading (or lateral overload). The objective of this present study is to: (1) develop design criteria and equations for the SC connections; and (2) verify the criteria and equations using computational analyses.

To advance the knowledge of behavior and design of traffic sign supporting structures with SC connections, an SC connection were conceptually designed for an existing dynamic-message-sign-supporting long-span bridge-mounted-type structure located in Montgomery, Alabama; computational models were built; and nonlinear analyses were conducted. Based on analysis results, conclusions can be drawn as follows:

- The developed criteria and equations are adequate for traffic sign supporting structures with SC connections to rock at the base, and to dissipate wind-imposed energy using

supplemental devices, rather than using damage to structural members as the major resource of energy dissipation.

- Traffic sign supporting structures using SC connections can be designed to act like conventional structures under the design wind load or smaller.
- The initiation of the rocking motion can be controlled to occur at the design target and enable energy to be dissipated by non-damage-based supplemental ED devices.
- Using the developed design criteria and equations, SC connections can be designed to dissipate the appropriate amount of energy as targeted while achieving self-centering behavior.
- Traffic sign supporting structures can be designed to self-center without permanent lateral displacement.
- Traffic sign supporting structures using SC connections outperform conventional structures in terms of damage inhibition, collapse prevention potential, stabilized ductility, and resilience.

9 FUTURE WORKS

This study is the first phase of the research developing SC connections for traffic sign supporting structures. The study has exploratorily developed and numerically verified design criteria and equations for the SC connections, and fulfilled the proposed project tasks for the phase I research.

Verification by computational analyses is essential and cost-effective, but not sufficient for practical applications. Thus, for the SC connections to be used in practice, experimental studies and verification must be conducted (1) to develop construction details for joints among SC connections, existing frame members and supports, and (2) to further advance the knowledge of performance of the structures with SC connections; so that the potential of the SC connections for practical applications will not be prevented.

REFERENCES

AASHTO (2013) “Standard Specification for Structural supports for Highway Signs, Luminaires, and Traffic Signals.” AASHTO, Washington, DC.

Mazzoni S, McKenna F, Scott MH, Fenves GL. (2013) “Open System for Earthquake Engineering Simulation (OpenSees) User Command-Language Manual Version 2.4.” Available from <http://opensees.berkeley.edu/OpenSees/user/download.php>.